Journal of Applied Polymer Science

BSA imprinted polyethylene glycol grafted calcium alginate hydrogel microspheres

Jiangquan Liu, Xiaoguang Ying, Hongxun Wang, Xiao Li, Weiying Zhang
School of Chemical Engineering, Fuzhou University, Fuzhou 350108, China
Correspondence to: X. Ying (E-mail: yxg@fzu.edu.cn)

ABSTRACT: Polyethylene glycol grafted calcium alginate hydrogel microspheres are synthesized by ring-opening and addition reaction of epoxy chloropropane. FTIR, ^{13}C NMR, optical microscope, SEM, TG, and DSC are used for characterization. Swelling behaviors are studied and it is found that polyethylene glycol grafted calcium alginate microspheres are improved in anti-swelling properties. Protein-imprinted polyethylene glycol grafted calcium alginate hydrogel microspheres exhibit enhanced specific rebinding quantity (11.16 mg/g) and selective recognition properties (4.71 against BHb), towards target molecule in the presence of competing protein, compared with that of the unmodified samples (4.96 mg/g and 1.75, respectively). © 2016 Wiley Periodicals, Inc. J. Appl. Polym. Sci. **2016**, *133*, 43617.

KEYWORDS: biomaterials; gels; grafting; molecular recognition; proteins

Received 13 December 2015; accepted 9 March 2016
DOI: 10.1002/app.43617

INTRODUCTION

Hydrogels containing numerous hydrophilic groups could absorb water from 10% to 20% up to thousands of times of their dry weight. Since crosslinked 2-Hydroxyethyl Methacrylate (HEMA) was firstly synthesized by Wichterle and Lim in 1960, hydrogel has been of great interest to scientists for many years because of its hydrophilic character and biocompatibility.[1–3] Nowadays, hydrogel is widely applied in a lot of fields including drug delivery, sensing applications, tissue engineering and molecular imprinting.[4–8]

Molecularly imprinted polymers (MIPs) are crosslinked polymeric networks designed to recognize target molecule specifically. Nowadays, MIPs have been successfully applied to recognize small molecules such as sugars, metal ions, or amino acids.[9–12] However, there are still challenges for protein recognition because of large size and complex conformation. But it could be overcome to some extent by adopting hydrogels as imprinted materials. Hydrogel with large mesh size and water content helps to maintain the conformation stability of proteins.

Protein imprinted polymers based on synthetic or natural hydrogels have been studied over the past decades. Alginate is one kind of natural polysaccharides which can form hydrogel structure with ionic crosslinking. Calcium alginate (CaA) is a typical example of hydrogels with stable "egg-box" structure and it has been considered as an ideal candidate for protein imprinting. Nowadays, lots of researches have been attracted by CaA because of its excellent biocompatibility, nontoxicity, and low cost.[13–15] However, alginate hydrogels easily erode and disintegrate because of ion exchanging.[16] Many modifications including physical or chemical procedures towards alginates have been carried out and some remarkable improvements have been achieved. Physical methods usually include blending with other inorganic or organic constituents while chemical methods are grafting modification, semi-interpenetrating, and interpenetrating.[17–19]

Polyethylene glycol (PEG) has been widely used in many fields for their satisfying properties in biomedical applications and selective recognition of protein.[20–22] In our research, PEG is grafted onto the glucoside hydroxyl groups of sodium alginate (SA) by ring-opening and addition reaction of epoxy chloropropane (ECH). PEG grafted calcium alginate microspheres are then prepared by Ca^{2+} crosslinking. FTIR, ^{13}C NMR, SEM, optical microscope, TG, and DSC are applied to characterize the chemistry structure and micro scale morphology. Swelling behaviors are investigated with the variation of pH. Moreover protein-imprinted PEG grafted calcium alginate hydrogel microspheres are prepared and investigated and the specific rebinding properties are assessed by comparing with the results presented in the reports up to date.

EXPERIMENTAL

Materials

SA was obtained from Sinopharm Chemical Reagent, China. PEG600 (600: molecular weight) was obtained from Tianjin Chemical Reagent Factory. ECH was obtained from Aladdin Reagent, China. Bovine serum albumin (BSA, pI = 4.7, $M_w = 66$

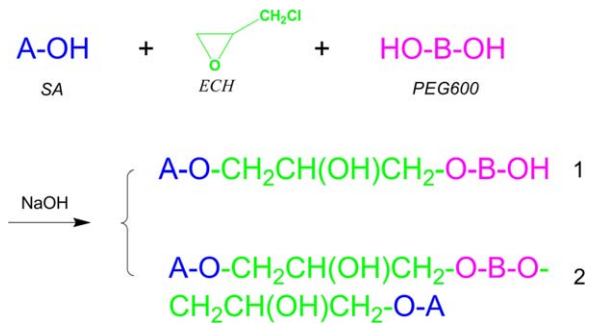

Figure 1. Main Chemical reaction between SA and PEG600. The reaction may probably follow the route 1 or 2. [Color figure can be viewed in the online issue, which is available at wileyonlinelibrary.com.]

kDa), bovine hemoglobin (BHb, pI = 6.9, M_w = 65 kDa) were supplied by Sigma-Aldrich. All reagents are commercially available and used without further purification.

Preparation Methods

The grafting reaction was carried out in a 100 mL three-necked flask by first dissolving 1.5 g SA in 60 mL distilled water followed by the addition of PEG600. pH was controlled at 10 by NaOH and then ECH was added. The three-necked flask was placed in a thermostatic bath at desired temperature for 4 h with magnetic stirring. At last, PEG600 grafted SA (SA-*g*-PEG600) was synthesized in aqueous solution by ring-opening reaction and addition reaction of ECH as shown in Figure 1.

PEG 600 grafted calcium alginate (CaA-*g*-PEG600) microspheres were formed by dropping the SA-*g*-PEG600 solution into 50 mL 1.5–2.5 wt % $CaCl_2$ solution and incubated for 2 h. Then the microspheres were subjected to Soxhlet extraction with a solution consisting of water and acetone (V:V = 9:1) at 75 °C for 12 h and dried under vacuum at 50 °C for 24 h. CaA microspheres were synthesized under the same condition as above, except the absence of PEG600, ECH and NaOH.

Grafting ratio (GR) is estimated by the equation as follows:

$$GR\ (\%) = (W_2 - W_1)/W_1 \times 100 \quad (1)$$

W_1 and W_2 are the weight of dry CaA and CaA-*g*-PEG600 microspheres, respectively. Samples of different grafting ratios are shown in Table I. The sample with highest grafting ratio is chosen for FTIR, ^{13}C NMR, optical microscope, SEM, TG, and DSC characterization.

BSA solution (2.5 mg/mL, 10 mL) was mixed with SA-*g*-PEG600 solution and allowed self-assembling under pH = 6.5 at room temperature for 4 h. Considering the molecular weight of SA glycoside unit and BSA, the mole ratio of BSA to COOH is nearly 0.055:1. Then protein-imprinted CaA-*g*-PEG600 microspheres were prepared by dropping the mixture from an injector into 2 wt % $CaCl_2$ aqueous solution and incubating for 2 h. The microspheres were eluted by a mixture of 0.2 wt % NaOH solution and 5 wt % sodium dodecyl sulfate (SDS) solution. The concentration of BSA was determined by UV/vis spectrophotometer at 279 nm at room temperature until no protein was detected in the eluant. The template removal was quantified via the ratio of BSA in eluant to the total template amount, which was up to 92% and different eluted results are shown in Table II. Nonimprinted polymers (NIPs) are synthesized under the same condition as above, except the absence of BSA template. The whole preparation procedure above is shown in Scheme 1.

Measurements

FTIR spectrums were taken by using FTIR (Spectrum 2000 FTIR, PerkinElmer, US) between 800 and 3200 cm^{-1}. ^{13}C NMR solid state nuclear spectrums were obtained on NMR spectrometer (AVANCEIII 500, Bruker, Swiss). Optical microscope photographs were taken by optical microscope (ZSA302, Chongqing Photoelectric Instrument. China). Microscope morphology photographs were taken by scanning electron microscope (HIROX SH-4000M, China). TG and DSC curves were obtained on comprehensive thermal analyzer (STA409PG, Netzsch. Germany). Protein concentration was detected by UV/vis spectrophotometer (Cary50, The Southeast Chemical Instrument, China).

Swelling Behaviors Test with pH (SD-pH)

A given amount of dry gel microspheres (W_0) was placed in the solution with different pH and the weight (W_t) was recorded when the swelling reaches equilibrium. Each sample was measured three times and the average weight was calculated. The swelling degree (SD) percentage is defined as the following equation:

$$SD\ (\%) = (W_t - W_0)/W_0 \times 100 \quad (2)$$

Protein Rebinding Tests

The rebinding experiments were all carried out at room temperature. Exactly weighted 1.0 g wet imprinted and nonimprinted microspheres were placed in test tubes containing protein solution (2.5 mg/mL, 10 mL) at various pH. The equilibrium rebinding quantity (Q_e) is calculated using the following equation:

Table I. Synthesis Details of CaA-*g*-PEG600

Sample	Weight of SA (g)	Weight of PEG (g)	Weight of ECH (mL)	Weight of NaOH (g)	Reaction time (h)	GR (%)
CaA	1.5	0	0	0	0	0
CaA-g-PEG600(1)	1.5	1.0	0.3	0.2	2.5	32
CaA-g-PEG600(2)	1.5	1.0	0.5	0.2	2.5	37
CaA-g-PEG600(3)	1.5	1.5	0.3	0.2	2.5	58
CaA-g-PEG600(4)	1.5	1.5	0.5	0.2	2.5	72

Table II. Template Removal Results of Various Eluants

Eluant	Template removal (%)
H_2O	29
Methanol-Acetic acid (V:V = 3:7)	63
Tris-HCl solution	77
0.2 wt % NaOH-5 wt % SDS solution	92

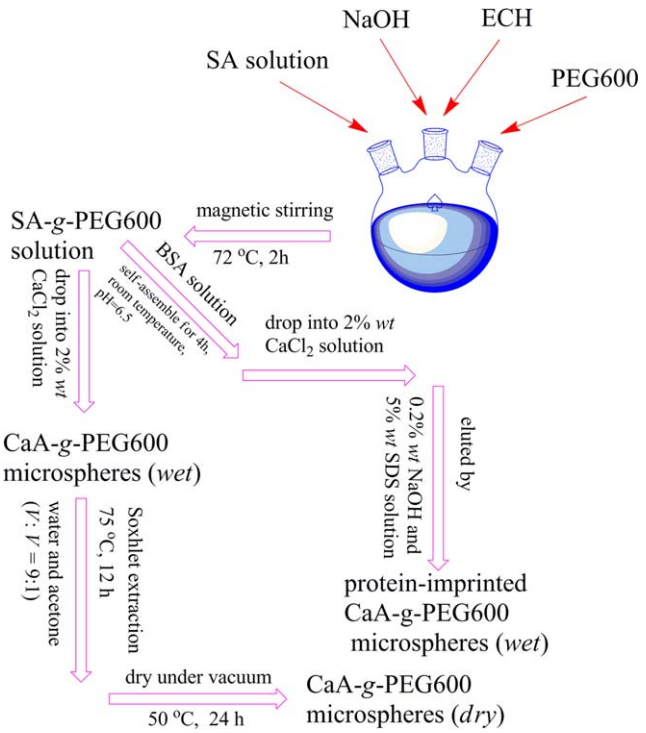

Scheme 1. Main plan of synthesis [Color figure can be viewed in the online issue, which is available at wileyonlinelibrary.com.]

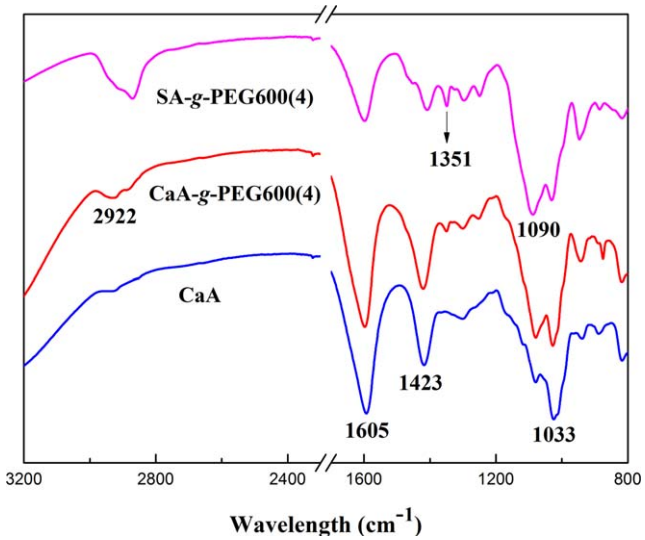

Figure 2. FTIR spectrums of CaA, SA-*g*-PEG600(4), and CaA-*g*-PEG600(4). [Color figure can be viewed in the online issue, which is available at wileyonlinelibrary.com.]

$$Q_e = (C_0 - C_e)V/m \quad (3)$$

C_0 and C_e are initial and equilibrium concentrations of protein, respectively; V is the volume of protein solution, and m is the mass of microspheres. The recognition ability is evaluated by imprinting efficiency (IE), which is calculated by the following equation:

$$\mathrm{IE} = Q_M/Q_N \quad (4)$$

Q_M and Q_N are protein rebinding quantities of MIPs and NIPs, respectively.

The selectivity of imprinted microspheres is evaluated by static distribution coefficient K_D and separation factor α, which are calculated using the following equations:

$$K_D = Q_e/C_e \quad (5)$$

$$\alpha = K_{D1}/K_{D2} \quad (6)$$

K_{D1} and K_{D2} are static distribution coefficients of template and competing molecules, respectively. The concentration of competing protein BHb is measured by UV/vis spectrometer at 405 nm.

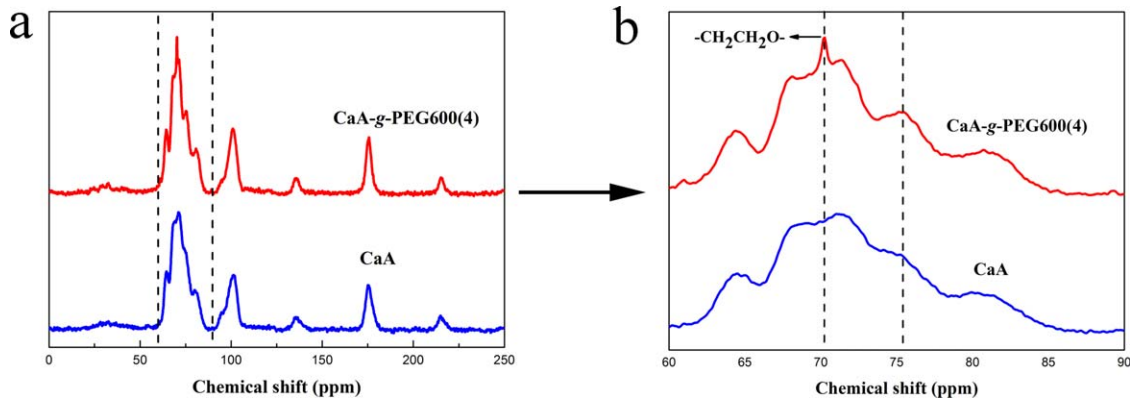

Figure 3. (a) ^{13}C NMR spectrums of CaA and CaA-*g*-PEG600(4); (b) magnification of "(a)" within 60 and 90 ppm. [Color figure can be viewed in the online issue, which is available at wileyonlinelibrary.com.]

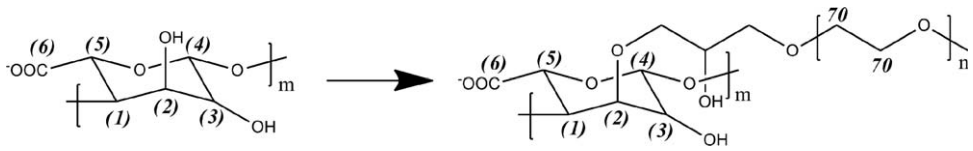

Figure 4. Repeating units of (a) CaA and (b) CaA-*g*-PEG600.

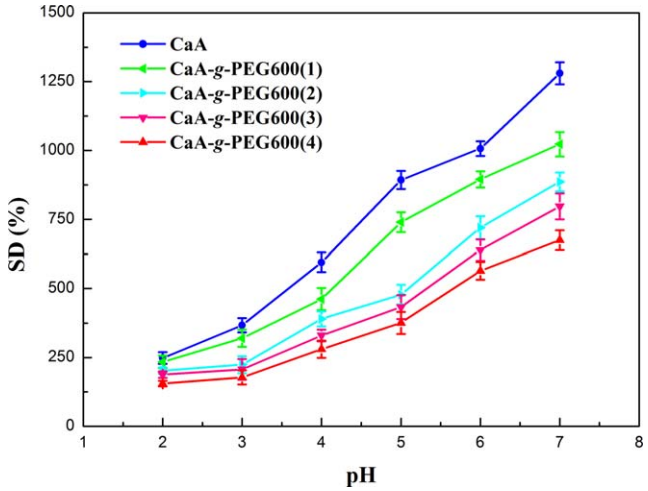

Figure 5. SD-pH of CaA and CaA-*g*-PEG600 microspheres. [Color figure can be viewed in the online issue, which is available at wileyonlinelibrary.com.]

RESULTS AND DISCUSSION

FTIR

Samples were dried under vacuum before taking FIIR test. FTIR spectrums of CaA, SA-*g*-PEG600(4), and CaA-*g*-PEG600(4) are shown in Figure 2. New peaks of SA-*g*-PEG600(4) and CaA-*g*-PEG600(4) are spotted for typical C–O–C stretching vibration peak is located at 1090 cm^{-1} and C–H bending vibration peak at 1351 cm^{-1}. These two stronger peaks of SA-*g*-PEG600(4) are mainly because of the free PEG600 contained in the sample. Typical peak of $–CH_2$ stretching vibration at 2922 cm^{-1} is weakened in CaA-*g*-PEG600(4) sample because free PEG600 was eluted in the process of dropping SA-*g*-PEG600 solution into $CaCl_2$ solution. In all samples, typically asymmetric and symmetric stretching vibration peaks of the alginate carboxylate group are located at 1605 and 1423 cm^{-1}. The peak of 1033 cm^{-1} belongs to C–O stretching vibration of the glucoside rings.[23] These give an evidence that PEG600 is grafted onto CaA.

^{13}C NMR

^{13}C NMR was used to further confirm a successful grafting reaction between the hydroxyl groups and ECH. ^{13}C NMR spectrums and chemical structures of CaA and CaA-*g*-PEG600(4)

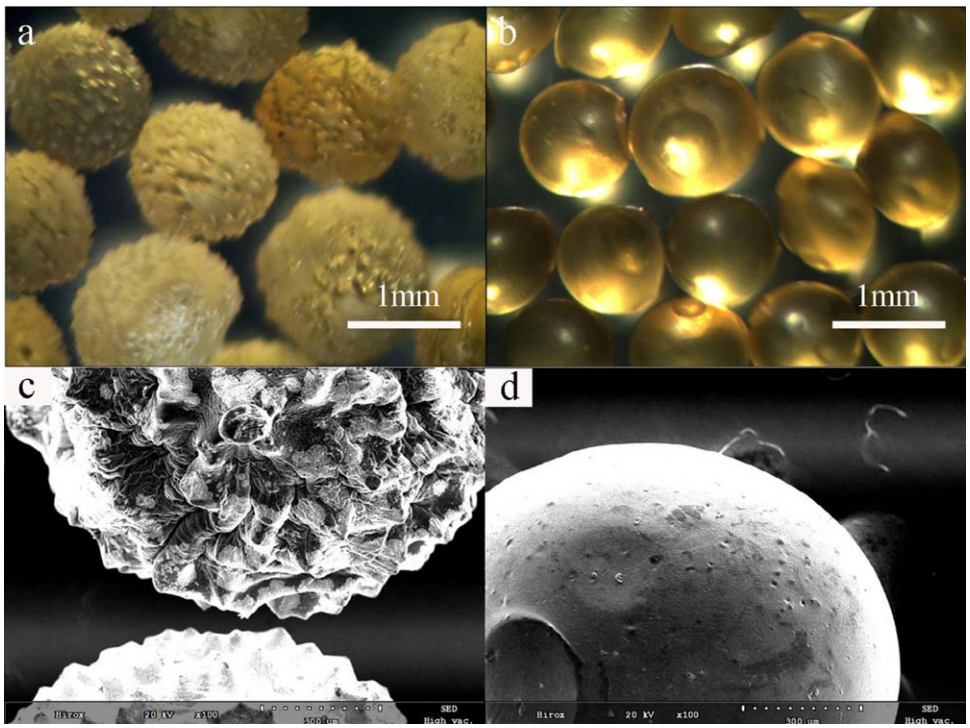

Figure 6. Optical microscope images of (a) CaA and (b) CaA-*g*-PEG600(4) microspheres; SEM images of (c) CaA and (d) CaA-*g*-PEG600(4) microspheres. The scale bar of SEM is 300 μm. [Color figure can be viewed in the online issue, which is available at wileyonlinelibrary.com.]

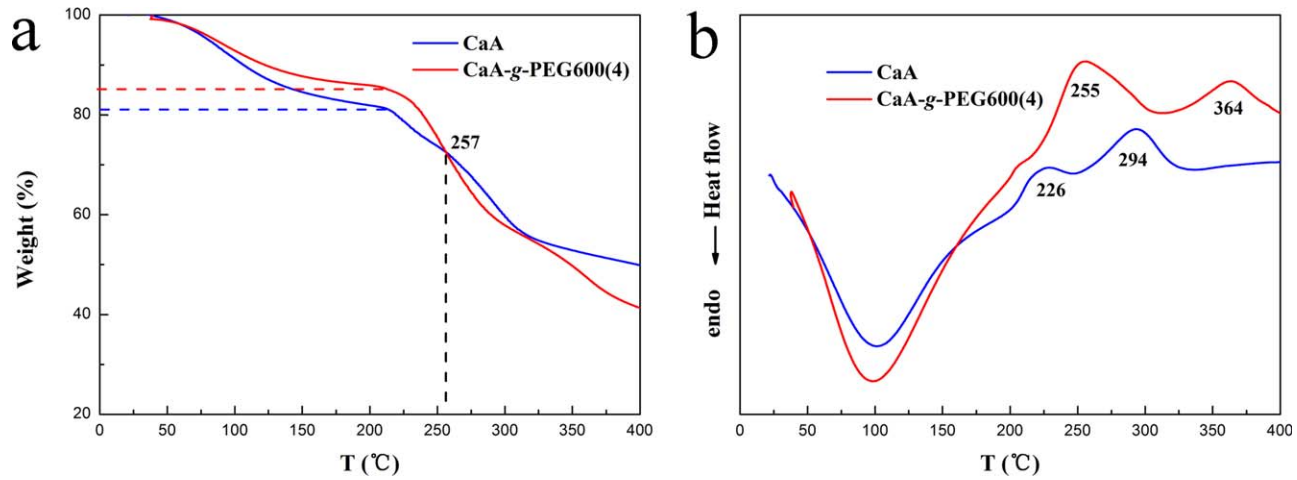

Figure 7. (a) TG curves of CaA and CaA-*g*-PEG600(4); (b) DSC curves of CaA and CaA-*g*-PEG600(4). [Color figure can be viewed in the online issue, which is available at wileyonlinelibrary.com.]

are shown in Figures 3 and 4. The peaks around 175 ppm are because of the $-COO^-$ of alginate.[24] The peaks of carbons on the glucoside ring of alginate [C(1∼5)] shift from 71 to 101 ppm. The chemical shift of C(2) around 75 ppm is strengthen in CaA-*g*-PEG600(4) because of the grafted PEG side chains. Also a very strong peak of 70 ppm which belongs to the C of PEG600 is clearly seen in CaA-*g*-PEG600(4).[25]

Swelling Behaviors

Swelling test helps to study the interaction between groups and water. SD-pH curves are shown in Figure 5. SDs of all samples are low when pH $\leq$ 3 because most of the $-COO^-$ groups of CaA are transformed into –COOH.[26,27] Intermolecular hydrogen bonds are formed between the carboxylate groups of CaA and predominate over the polymer–H_2O interactions. Therefore swelling behavior is hindered. However, as the pH increases, most of the –COOH groups tended to dissociate into $-COO^-$, which leads to electrostatic repulsion between the polymer chains. Therefore water molecules diffuse into the microspheres more easily. SDs of CaA-*g*-PEG600 microspheres are similar to CaA microspheres. But CaA-*g*-PEG600 microspheres with smoothing surfaces absorb less water than CaA microspheres with wrinkled structures (as seen in the following optical microscope and SEM pictures).

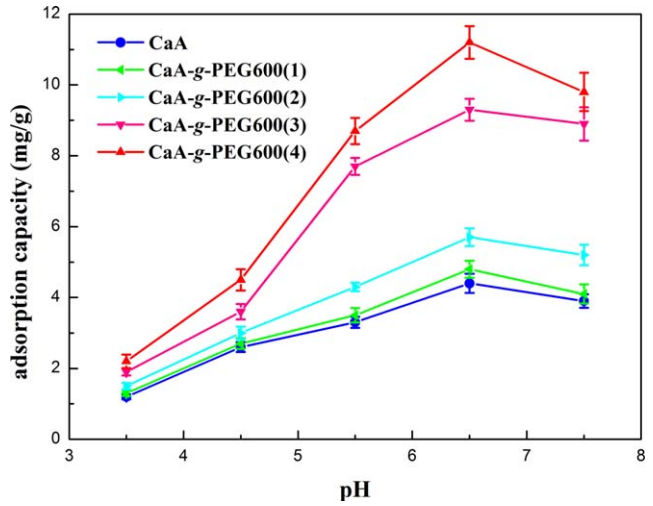

Figure 8. Imprinted CaA-*g*-PEG600 samples for BSA adsorption with various pH. [Color figure can be viewed in the online issue, which is available at wileyonlinelibrary.com.]

Optical Microscope and SEM

The morphology of microspheres reveals the influence of grafting on the structure of hydrogel samples. Microspheres are dried under vacuum and then sampled for optical microscope and SEM characterization. As is shown in Figure 6, the size of dry CaA-*g*-PEG600(4) microsphere is smaller than CaA microsphere. CaA-*g*-PEG600(4) microsphere exhibits a bright, semitransparent, and smoothing surface while CaA microspheres with a wrinkled surface. These pictures indicate that grafting reaction has changed the structure of hydrogel.

TG and DSC

In order to study thermal stability of samples, thermal properties are investigated by TG and DSC (10 K/min, Ar) and the curves are given in Figure 7(a,b). Weight losses in the first step of TG for CaA and CaA-*g*-PED600(4) are because of the elimination of bond water. It could be clearly seen that CaA-*g*-PEG600(4) is relatively stable within a temperature span from 25 °C to 257 °C, which is adequate for practical adsorption in aqueous solution. In DSC curves of CaA, the exothermic peaks appear at 226 °C and 294 °C because of the decomposition of $-COO^-$ and –OH, respectively.[28,29] As for CaA-*g*-PEG600(4) the exothermic peaks shift to higher temperature at 255 °C and 364 °C. The results show that more thermal stabilized structure is formed in CaA-*g*-PEG600(4) gels.

Rebinding Specificity

Rebinding specificity reflects whether a material an ideal matrix or not. In our work, careful tests were carried out to study the rebinding specificity according to the variables such as GR, pH, and Ca^{2+} concentration. Competitive adsorption was also carried out between BSA and BHb in order to investigate the rebinding selectivity.

Table III. IE and α of Single and Binary Protein Tests

Calcium concentration		CaA microspheres		CaA-*g*-PEG600(4) microspheres		CaA with free PEG600 microspheres	
		IE for BSA	α against BHb	IE for BSA	α against BHb	IE for BSA	α against BHb
1.5 wt % $CaCl_2$ solution	single	1.36	1.65	2.23	3.97	1.41	1.98
	binary	1.27	1.40	2.12	3.56	1.37	1.67
2 wt % $CaCl_2$ solution	single	1.42	1.75	**2.78**	**4.71**	1.57	2.21
	binary	1.35	1.45	2.56	3.67	1.43	2.03
2.5 wt % $CaCl_2$ solution	single	1.40	1.72	2.71	4.65	1.53	2.07
	binary	1.33	1.41	2.49	3.62	1.39	1.99

Imprinted microspheres with different GRs are applied in adsorption tests under various pH. As is shown in Figure 8, all of the microspheres exhibit the maximum adsorption at pH =6.5, the same with the pre-assembling surrounding, at which the imprinted cavity and specific sides' configuration match BSA to the best extend. CaA-*g*-PEG600(4) microspheres have the highest adsorption within testing pH span (2.5–7.5). Therefore it is presumed that the grafted PEG chains may have contributed to the adsorption of BSA. As CaA-*g*-PEG600(4) possesses the best specific adsorption

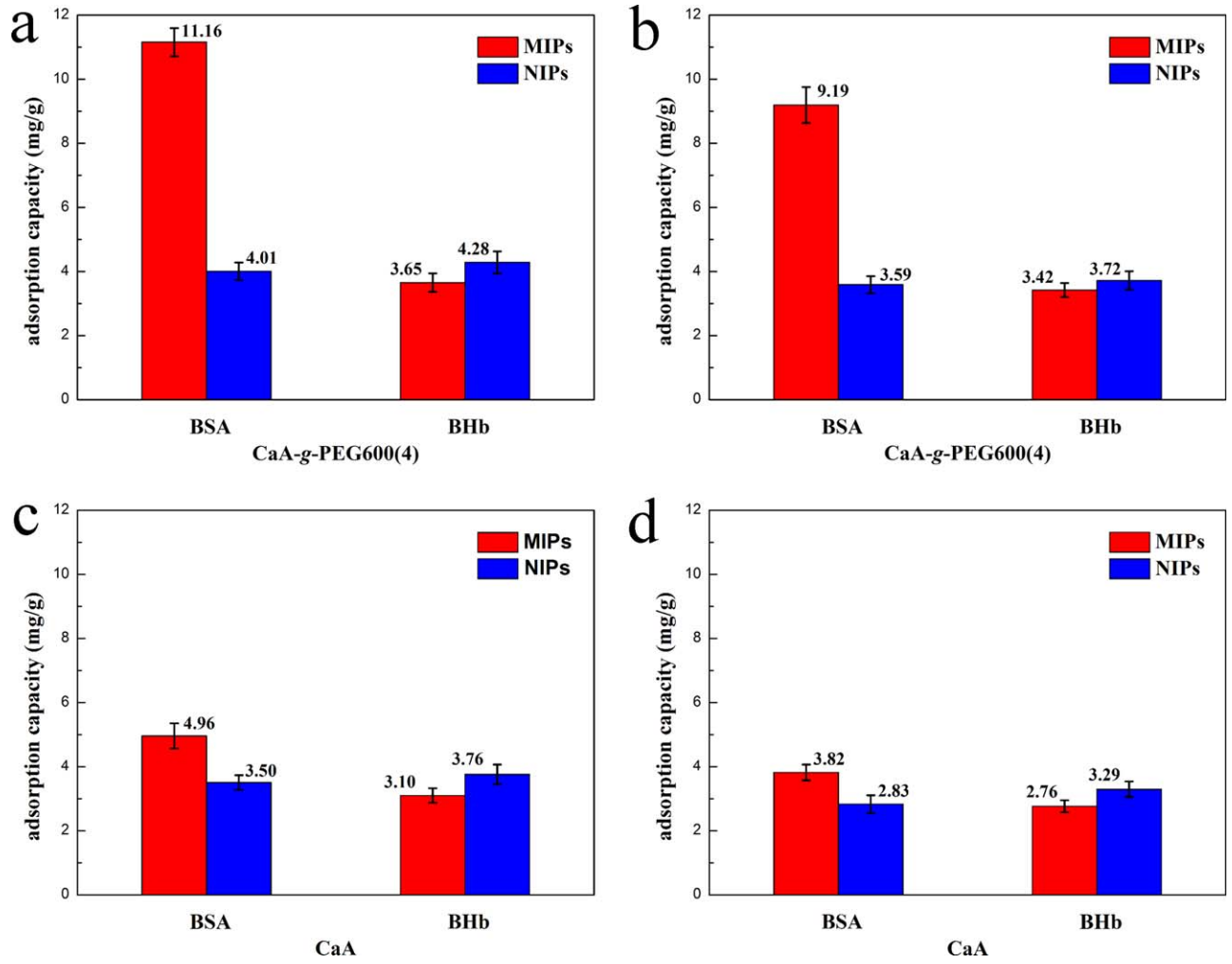

Figure 9. Adsorption capacities of proteins on the CaA-*g*-PEG600(4) and CaA microspheres in single (a,c) and binary (b,d) protein competitive adsorption tests. [Color figure can be viewed in the online issue, which is available at wileyonlinelibrary.com.]

Table IV. Part of Relevant Works during 2008 to 2015

Group	Material	Template protein (A)/ Competitive protein(B)	M_w (kDa)		pI		IE	α
			A	B	A	B		
Cheng *et al.*[30]	Alginate-based hydrogel	BSA/Glo	66	160	4.8	6.8	3.47	3.56
Cheng *et al.*[31]	Alginate-based hydrogel	EA/-	45	—	4.7	—	1.97	—
Cheng *et al.*[32]	Agarose-based hydrogel	BSA/Hb	66	68	4.8	6.7	2.16	2.82
Kubo *et al.*[33]	PEG-based hydrogel	Lyz/Cy c	14	12	10.8	10.2	8.60	3.91
Searson *et al.*[34]	PAM-based hydrogel	MBP/BSA	41	66	4.4	4.8	3.83	3.75
Zhao *et al.*[35]	PAM-based hydrogel	BSA/BHb	67	64	4.9	6.9	3.30	2.00
Ying *et al.*[36]	Alginate-based hydrogel	BSA/OVA	66	46	4.7	4.7	1.80	7.23
Caykara *et al.*[37]	NIPA-based hydrogel	Fbg/BSA	340	67	5.8	4.8	2.45	3.66
Li *et al.*[38]	PAM-based hydrogel	BHb/BSA	66	67	6.7	4.9	4.95	3.81
Ye *et al.*[39]	PAM-based hydrogel	Hb/BSA	65	69	6.8	4.9	4.17	2.23
Ying *et al.* (this work)	Alginate-based hydrogel	BSA/BHb	66	65	4.7	6.9	2.78	4.71

Bovine hemoglobin (BHb), bovine serum albumin (BSA), cytochrome c (Cy c), egg white albumin (EA), fibrinogen (Fbg), hemoglobin (Hb), lysozyme (Lyz), maltose binding protein (MBP), N-isopropylacrylamide (NIPA), ovalbumin (OVA), polyacrylamide (PAM), r-globulin (Glo).

among all of the samples, it is applied in the following selective rebinding tests.

BHb is chosen as competitive protein to run a single rebinding test. Rebinding capacities (RCs) of all microsphere samples are presented in Figure 9 and detailed results are listed in Table III. It is found that CaA with free PEG600 microsphere has a close α to CaA microsphere. The main reason is that PEG600 is well water soluble and diffuse into incubating solution during microspheres forming without grafting reaction, which is confirmed by FTIR analysis. As an ionic crosslinker, Ca^{2+} affects the cave dimension as well as the imprinting property. As can be seen in Table III, IE as well as α reaches maximum when the CaA-g-PEG600(4) microspheres are formed in 2 wt % $CaCl_2$ solution. Therefore in the following test, 2 wt % $CaCl_2$ solution is chosen as the crosslinking agent. CaA-*g*-PEG600(4) microspheres exhibit rebinding property with IE of 2.78 and RC of 11.16 mg/g towards BSA. α is 4.71 for BHb, indicating an appreciable selectivity towards the template BSA. Also binary protein competitive adsorption tests are carried out. In Figure 9(b), it is noticed that in the mixture solution of BSA and BHb, MIPs still rebind more BSA than BHb with α of 3.67. IE and α obtained from binary system are lower than that from single protein systems. This is considered as the result of the interaction between different proteins. RCs, IE, and α of CaA microspheres in single and binary protein tests are lower than those of CaA-*g*-PEG600(4) microspheres as seen in Figure 9(c,d).

With the aim of a comprehensive overview of the progress in this work and other related researches, recently published achievements concerning protein imprinted hydrogel materials are listed in Table IV. Lysozyme-imprinted PEG-based hydrogel prepared by Kubo *et al.* possesses the remarkable IE which could reach to 8.60 with α of 3.91 against Cy c.[33] It is suggested

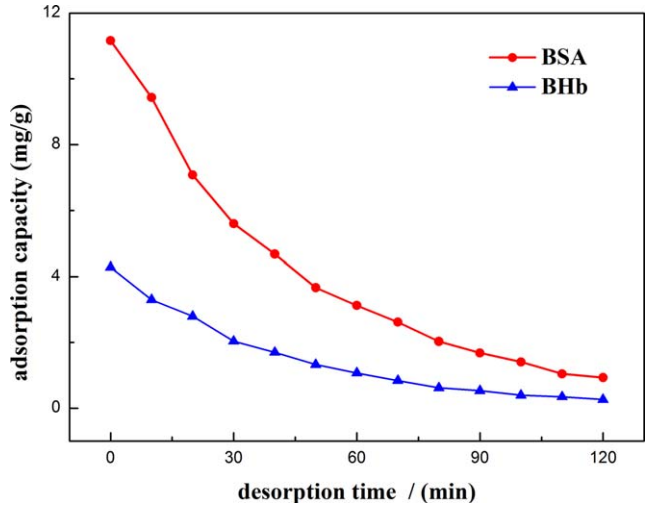

Figure 10. Desorption of BSA and BHb on CaA-*g*-PEG600(4) MIPs. [Color figure can be viewed in the online issue, which is available at wileyonlinelibrary.com.]

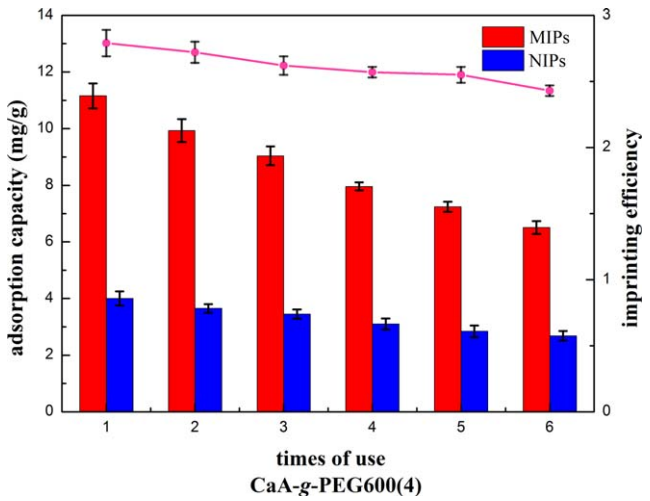

Figure 11. Repeated performance of CaA-*g*-PEG600(4) for BSA adsorption. [Color figure can be viewed in the online issue, which is available at wileyonlinelibrary.com.]

that flexible network of PEG and the suppression of nonspecific ionic interaction contribute to the selective adsorption of protein. BSA-imprinted polyacrylamide-based hydrogel has IE of 3.83 and α of 3.75 in the study of Searson *et al.*[34] As for the natural polysaccharide systems, BSA-imprinted alginate-based hydrogel with better biocompatibility prepared by Cheng *et al.* exhibits considerable IE of 1.97 by forming emulsion porous structure.[31] Then it is further explored by Ying *et al.* with IE of 1.80 and α up to 7.23 through introducing polyurethane grafting segments.[36] All of the works have demonstrated that protein imprinted hydrogel is a promising material for the selective adsorption and separation of protein. The results presented in this article takes the advantaged of PEG, a water-soluble polymer with biocompatibility and low toxicity, in forming alginate-based hydrogel with lower SD. Meanwhile the ionic crosslinking ability and large mesh size is preserved, which is favorable of template stability and site accessibility.

Desorption of Protein

Desorption of protein is also studied to make a good explanation about the mechanism of BSA binding. Desorption curve of protein [CaA-*g*-PEG600(4) MIPs] is shown in Figure 10. It is seen that target protein BSA decreases faster as the time increases than the competitive protein BHb. The main reason is that the rebinding of protein consists of specific and nonspecific adsorption (as seen in the Graphical abstract). It is inferred that both specific and nonspecific adsorption are effective in CaA-*g*-PEG600(4) MIPs for target protein BSA while only nonspecific adsorption contribute to the rebinding of competitive protein BHb.

Recycle Performance

Recycle performance of CaA-*g*-PEG600(4) microspheres for BSA adsorption is shown in Figure 11. RCs of MIPs and NIPs as well as IE for BSA decrease in the recycle. The main reason is that the process of elution could destroy the specific sites and cavity structures in the hydrogel. Moreover the template removal at each recycle is about 92%, which is also a limit to RC and IE of reused microspheres. Nevertheless, MIPs still exhibit higher RC for BSA than NIPs. After five recycles, BSA RC of CaA-*g*-PEG600(4) microspheres is 6.51 mg/g, approx. 58% of the initial amount. Meanwhile, IE for BSA is 2.43, approx. 87% of the initial amount. RC of MIPs consists of specific recognition and nonspecific adsorption. The deterioration of imprinted structure at eluting results a more remarkable decrease in the specific recognition and imprinting efficiency of MIPs than NIPs.

CONCLUSIONS

CaA-*g*-PEG microspheres are prepared and FTIR and ^{13}C NMR give evidences that PEG has been grafted onto CaA. Modified CaA microspheres have more smoothing surfaces than CaA microspheres as seen under optical microscope and SEM. CaA-*g*-PEG600 microspheres exhibit lower swelling degree than CaA microspheres. CaA-*g*-PEG MIPs rebind more BSA than NIPs, with IE of 2.78 for BSA and α of 4.71 for BHb. Recycle test suggests relative stability in CaA-*g*-PEG gels when used as specific adsorption materials for protein. In virtue of the remarkable rebinding specificity and selectivity of the hydrogel microspheres, they are of prospecting applications such as protein separation and purification, cancer early diagnosis by secretion biomarkers online detection, protein drug delivery and target therapy.

ACKNOWLEDGMENTS

The authors thank the support of Fuzhou University Science Technology Development Fund (2014-XQ-23), China Postdoctoral Science Foundation (2012M511439), Talent Foundation of Fuzhou University (XRC-1011), Science and Technology Project (A class) of Fujian Provincial Education Department (JA11021).

REFERENCES

1. Wang, J. Y.; Cao, Y.; Feng, Y.; Yin, F.; Gao, J. P. *Adv. Mater.* **2007**, *19*, 3865.
2. Zhao, X.; Cui, W. *Mater. Today* **2015**, *18*, 56.
3. Satarkar, N. S.; Zach Hilt, J. *Acta Biomater.* **2008**, *4*, 11.
4. Hamidi, M.; Azadi, A.; Rafiei, P. *Adv. Drug Deliv. Rev.* **2008**, *60*, 1638.
5. Qiu, Y.; Park, K. *Adv. Drug Deliv. Rev.* **2012**, *64*, 49.
6. Buenger, D.; Topuz, F.; Groll, J. *Prog. Polym. Sci.* **2012**, *37*, 1678.
7. Ren, K.; He, C.; Xiao, C.; Li, G.; Chen, X. *Biomaterials* **2015**, *51*, 238.
8. Byrne, M. E.; Salian, V. *Int. J. Pharm.* **2008**, *364*, 188.
9. Okutucu, B.; Onal, S. *Talanta* **2011**, *87*, 74.
10. Hande, P. E.; Samui, A. B.; Kulkarni, P. S. *Sci. Pollut. R.* **2015**, *22*, 7375.
11. He, J.; Chen, J. P. *Ind. Eng. Chem. Res* **2014**, *53*, 20223.,
12. Liu, X. Y.; Fang, H. X.; Yu, L. P. *Talanta* **2013**, *116*, 283.
13. Zeeb, B.; Saberi, A. H.; Weiss, J.; McClements, D. J. *Soft Matter* **2015**, *11*, 2228.
14. Popeski-Dimovski, R. *Carbohydr. Polym.* **2015**, *123*, 146.
15. Lee, K. Y.; Mooney, D. J. *Prog. Polym. Sci.* **2012**, *37*, 106.
16. Ying, X.; Qi, L.; Li, X.; Zhang, W.; Cheng, G. *J. Appl. Polym. Sci.* **2013**, *127*, 3898.
17. Rani, P.; Mishra, S.; Sen, G. *Carbohydr. Polym.* **2013**, *91*, 686.
18. Samanta, H. S.; Ray, S. K. *Carbohydr. Polym.* **2014**, *99*, 666.
19. Yang, J.; Chen, J.; Pan, D.; Wan, Y.; Wang, Z. *Carbohydr. Polym.* **2013**, *92*, 719.
20. Cole, A. J.; David, A. E.; Wang, J.; Galban, C. J.; Hill, H. L.; Yang, V. C. *Biomaterials* **2011**, *32*, 2183.
21. Wang, X.; Partlow, B.; Liu, J.; Zheng, Z.; Su, B.; Wang, Y.; Kaplan, D. L. *Acta Biomater.* **2015**, *12*, 51.
22. Su, W. X.; Rick, J.; Chou, T. C. *Microchem. J.* **2009**, *92*, 123.
23. Abd El-Ghaffar, M. A.; Hashem, M. S. *Carbohydr. Polym.* **2013**, *92*, 2095.
24. Wang, J.; Ying, X.; Li, X.; Zhang, W. *Mater. Lett.* **2014**, *126*, 263.
25. Samiullah, M. H.; Reichert, D.; Zinkevich, T. *Macromolecules* **2013**, *46*, 6922.
26. Li, H.; Li, X. Y. *J. Fiber Bioeng. Inform.* **2009**, *2*, 168.

27. Abd El-Ghaffar, M. A.; Hashem, M. S.; El-Awady, M. K.; Rabie, A. M. *Carbohydr. Polym.* **2012**, *89*, 667.
28. Bekin, S.; Sarmad, S.; Gürkan, K.; Yenici, G.; Keçeli, G.; Gürdağ, G. *Polym. Eng. Sci.* **2014**, *54*, 1372.
29. Kadokawa, J.; Saitou, S.; Shoda, S. *Carbohydr. Polym.* **2005**, *60*, 253.
30. Zhao, K.; Cheng, G.; Huang, J.; Ying, X. *React. Funct. Polym.* **2008**, *68*, 732.
31. Ying, X.; Zhang, F.; Zhang, L.; Cheng, G. *J. Appl. Polym. Sci.* **2010**, *115*, 3516.
32. Ying, X.; Cheng, G.; Zhao, K. *Polym. Bull.* **2010**, *65*, 245.
33. Kubo, T.; Arimura, S.; Tominaga, Y.; Naito, T.; Hosoya, K.; Otsuka, K. *Macromolecules* **2015**, *48*, 4081.
34. Zayats, M.; Brenner, A. J.; Searson, P. C. *Biomaterials* **2014**, *35*, 8659.
35. Zhao, K.; Lin, B.; Cui, W.; Feng, L.; Chen, T.; Wei, J. *Talanta* **2014**, *121*, 256.
36. Li, L.; Ying, X.; Liu, J.; Li, X.; Zhang, W. *J. Appl. Polym. Sci.* **2015**, *132*, DOI: 10.1002/app.42140.
37. Çimen, D.; Akbulut, E.; Demirel, G.; Caykara, T. *React. Funct. Polym.* **2009**, *69*, 655.
38. Zhang, W.; Qin, L.; Chen, R. R.; He, X. W.; Li, W. Y.; Zhang, Y. K. *Appl. Surf. Sci.* **2010**, *256*, 3000.
39. Zhou, T.; Zhang, K.; Kamra, T.; Bülow, L.; Ye, L. *J. Mater. Chem. B* **2015**, *3*, 1254.